西南交通大学学报
第 54 卷 第 5 期
2019 年 10 月
JOURNAL OF SOUTHWEST JIAOTONG UNIVERSITY
Vol.54 No.5
Oct. 2019
ISSN: 0258-2724
DOI：10.35741/issn.0258-2724.54.5.37

MULTI -FOCUS IMAGE FUSION BASED ON STATIONARY WAVELET TRANSFORM AND PCA ON YCBCR COLOR SPACE

Alaa A. Abdullatif[a], Firas A. Abdullatif[a] , Amna al Safar[a]
[a]College of Education for pure science / Ibn Al-Haitham, University of Baghdad, Iraq

alaa.a.h@ihcoedu.uobaghdad.edu.iq, Firas.alobaedy@ihcoedu.uobaghdad.edu.iq,
amnaalsafar1@yahoo.com

Abstract

The multi-focus image fusion method can fuse more than one focused image to generate a single image with more accurate description. The purpose of image fusion is to generate one image by combining information from many source images of the same scene. In this paper, a multi-focus image fusion method is proposed with a hybrid pixel level obtained in the spatial and transform domains. The proposed method is implemented on multi-focus source images in YCbCr color space. As the first step two-level stationary wavelet transform was applied on the Y channel of two source images. The fused Y channel is implemented by using many fusion rule techniques. The Cb and Cr channels of the source images are fused using principal component analysis (PCA). The proposed method performance is evaluated in terms of PSNR, RMSE and SSIM. The results show that the fusion quality of the proposed algorithm is better than obtained by several other fusion methods, including SWT, PCA with RGB source images and PCA with YCbCr source images.

Keywords: Multi-focus image fusion, YcbCr color space, stationary wavelet transform, principal component analysis (PCA)

摘要：多焦点图像融合方法可以融合一个以上的聚焦图像，以生成具有更准确描述的单个图像。图像融合的目的是通过组合来自同一场景的许多源图像的信息来生成一个图像。本文提出了一种在空间域和变换域中获得混合像素水平的多焦点图像融合方法。该方法在 YCbCr 色彩空间中的多焦点源图像上实现。作为第一步，在两个源图像的 Y 通道上应用了两级平稳小波变换。通过使用许多融合规则技术来实现融合的 Y 通道。使用主成分分析（PCA）融合源图像的 Cb 和 Cr 通道。建议的方法性能根据 PSNR，RMSE 和 SSIM 进行评估。结果表明，与 SWT，具有 RGB 源图像的 PCA 和具有 YCbCr 源图像的 PCA 相比，该算法的融合质量要好于其他几种融合方法。

关键词: 多焦点图像融合，YcbCr 颜色空间，平稳小波变换，主成分分析（PCA)

I. INTRODUCTION

The sensor of imaging technology is affected by many factors of the imaging environment, for that the generated image may be displayed with noise and superficiality. Image fusion is defined as the process of producing a more accurate image by the fusion of multiple same scene images [1]. Multi-focus image fusion creates one image from two or more images that have same scenes, with these images having different focus points. The resultant image after the fused method has been applied has more information than the source images and is called the all-in-focus image [2]. Multi-focus image fusion has been used in different areas, such as remote

sensing, medical imaging, transportation, military applications and machine vision [3].

Pixel-level fusion uses the pixels of an image, being the lowest level of fusion when compared to others like feature level fusion and decision level fusion. Regarding the latter two, the fused image contains more information and is more conducive to computer processing and the human eye. There are two categories of pixel level fusion: image fusion methods based on the spatial and transform domains [4], [5].

The method in the spatial domain depends on selecting the pixels from the sources images to form the fused image. There are many methods used to determine the clear area of selecting pixels in the resource images like certain sharpness indicator, by window or by image segmentation of a specific size [6].

Several methods have been devised to perform image fusion with the transformation method, including wavelet transform, discrete wavelet transform (DWT), shift invariant wavelet transform (SIDWT), DCT based on average or DCT based on spatial frequency and non-subsampled contourlet transform (NSCT) [6], [7]. In the transformation domain image fusion methods are based on converting the original image into transformation coefficients. Then, these are fused by the appropriate fusion rules and finally, there is reconstruction of the fusion coefficients to obtain the fusion image [8].

In this paper, pixel level fusion is applied to special and transform domains. The source images, firstly, are converted into YCbCr color space and then two levels of SWT are applied to Y channel. Different fusion rules are used to fuse the SWT coefficient, while the PCA technique is used to fuse the Cb and Cr channels.

The rest of the paper is arranged as follows: The aim of the research is explained in section II. The basic theory is expounded in Section III. Section IV describes in detail the proposed image fusion algorithm. Parametric evaluation and the experimental results are discussed in Section V. Finally, Section VI presents the conclusions.

II. THE AIM OF THE RESEARCH

This research is aimed at proposing a method to enhance the scene of two different focus images by using two different appropriate rules to fuse approximation and detail sub-band of SWT for Y channels of the source images, while the PCA is used for fused Cb and Cr. For that, the research focuses on fused pixels in transform and spatial domains. This leads to better results according to many evaluation measurements because it uses the advantages of the two domains.

III. BASIC THEORY

The proposed method is based on the concept of many theories as follows:

A. YCbCr Color Space

The YCbCr color space can be considered as a scaled and offset version of YUV color space. The luminance component is represented by Y, while Cb and Cr are chromatic ones. The Cb component is the difference between the blue part of the RGB and the reference value, while Cr reflects the difference between the red part of RGB and the reference value. The advantage of YCbCr color space is that it can be used to separate the three channels and operate on each one separately without any effect. The equations that are used to convert RGB color space to YCbCr color space are as follows [10]:

$$\begin{pmatrix} y \\ Cb \\ Cr \end{pmatrix} = \begin{bmatrix} 0.257 & 0.564 & 0.098 \\ -0.148 & -0.291 & 0.439 \\ 0.439 & -0.368 & -0.071 \end{bmatrix} \begin{pmatrix} R \\ G \\ B \end{pmatrix} + \begin{bmatrix} 16 \\ 128 \\ 128 \end{bmatrix} \quad (1)$$

$$\begin{pmatrix} R \\ G \\ B \end{pmatrix} = \begin{bmatrix} 1.164 & 0 & 1.596 \\ 1.164 & -0.392 & -0.813 \\ 1.164 & 2.017 & 0 \end{bmatrix} \begin{pmatrix} Y - 16 \\ Cb - 128 \\ Cr - 128 \end{pmatrix} \quad (2)$$

where, *Y* has a range of [16-235], whilst *Cb* and *Cr* have ranges of [16-240].

B. Principal component analysis (PCA)

One of the pixel level fusion techniques, PCA, is widely used in image processing, machine learning, image fusion and many other applications. With PCA, the number of correlated variables are transformed into uncorrelated variables, which reduces the multidimensional data sets into lower dimensions for analysis. The technique calculates the weights for each source image according to an eigenvector. The eigenvector is produced by the largest eigenvalue of the covariance matrix of each source image. By choosing the highest eigenvalue vector to be the principle component the number of dimensions is reduced, thus leading to faster computation. Figure (1) shows the flow diagram for the PCA technique [11].

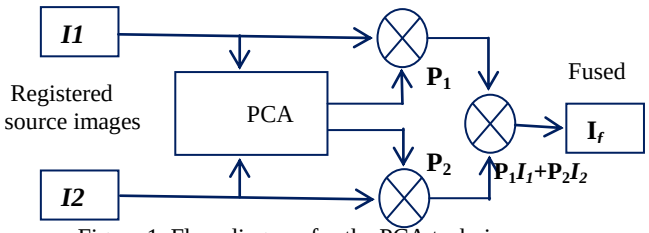

Figure 1. Flow diagram for the PCA technique

The steps of PCA analysis are as follows [12]:

- calculate the column vector based on the source image;
- create covariance C_{var} and correlation matrix A based on the data set of the input images x_1 and x_2, as in equations 3 and 4.

$$A = \begin{bmatrix} v_1 & c_{var}(1,2) \\ c_{var}(1,2) & v_2 \end{bmatrix} \quad (3)$$

$$C_{var} = \frac{(\sum(x_1 - \bar{x}_1) \times (x_2 - \bar{x}_2))}{N-1} \quad (4)$$

where v_1, and v_2, denote the variance, C_{var} (1,2) represents the covariance and N is the number of terms.

The eigenvalues can be calculated by solving:

$$Det|A - \lambda I| = 0 \quad (5)$$

where λ is the eigenvalue.

$$\begin{bmatrix} v_1 & c_{var}(1,2) \\ c_{var}(1,2) & v_2 \end{bmatrix} - \lambda_I = 0 \quad (6)$$

$$((v_1 - \lambda) \times (v_2 - \lambda)) \times C_{var}(1,2)^2 = 0 \quad (7)$$

The eigenvectors are calculated as follows:

$$[A - \lambda I] \times [X] = 0 \quad (8)$$

The co-ordinates for each point in the direction of the principal component are given by:

$$P_{cj} = a_{i1} y_1 + a_{i2} y_2 \ \ldots\ldots\ldots\ldots a_{in} y_n \quad (9)$$

where, a_1 is the coefficient of factor i , p_{cj} is the j^{th} principle component and y_1, y_2, ... y_n represent the coordinates of each data point.

C. Stationary Wavelet Transform

A discrete wavelet transform is time-variant and to reduce the poor directionality and translation variation, an undecimated approach has to be used, called a stationary wavelet transform (SWT). This has the properties of shift invariance and redundancy such that it is more efficient when compared to the traditional wavelet transform used for multi-scale transform methods and it is a non-redundant decomposition algorithm. The sub-image size in SWT does not decrease because it applies up-sampling filter instead of the down-sampling operation for that the most information of source images can be kept in the decomposed sub-images. SWT uses multi scale decomposition that can extract the small features in fine scales and the large ones in coarse scales. The presentation of images at each scale with SWT retains the native number of pixels throughout and it does not down sample the coefficients, which is why SWT was selected over DWT [13], [14]. The decomposition of the image in the SWT domain involves an approximation sub-band (LL) and detail sub-bands (LH, HL and HH), as shown in Figure 2 [15].

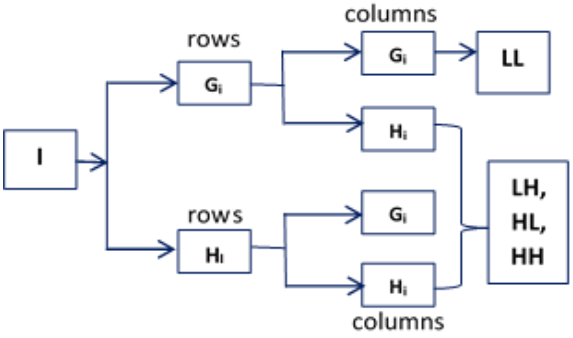

Figure 2. The decomposition of the image in the SWT domain

IV. THE PROPOSED METHOD

With the proposed method the source images are converted to YCbCr color spaces and then, a two-level SWT is applied to the Y channel of each image. Different fusion rules are used to fuse the SWT sub-band decomposition to get better results. The average rule is used to fuse the approximation sub-band (LL), while the detail sub-bands (LH, HL, and HH) are fused under another rule, PCA is used to fuse the Cb and Cr channels. Figure (3) shows the block diagram of the proposed method.

The steps of the proposed algorithm with fusion rules equations are shown in algorithm (1)

Algorithm (1): the proposed fusion
Input: two source multi focus images (A and B)
Output: fused image
Start
Step 1: transform source images from RGB to YCbCr color space.
Step 2: apply two-level stationary wavelet transform to the Y channel of A and B.
Step 3: fuse the approximation sub-band *LL* by the average rule as follows:

$$F_{LL} = (A_{LL} + B_{LL})/2 \quad (11)$$

Fuse the detail sub-bands LH, HL and HH as follows:

$$W_{LH} = \text{absolute } (A_{LH}) - \text{absolute } (B_{LH}) \quad (12)$$

$$F_{LH} = (W_{LH})\ (A_{LH}) + \text{not } (W_{LH})\ (B_{LH}) \quad (13)$$

W_{HL}=absolute (A_{HL})-absolute (B_{HL}) (14)

F_{LH}= (W_{HL}) (A_{HL}) + not (W_{HL}) (B_{HL}) (15)

W_{HH}=absolute (A_{HH})-absolute (B_{HH}) (16)

F_{HH}= (W_{HH})(A_{HH}) + not (W_{HH})(B_{HH}) (17)

Step 4: apply inverse SWT to F_{LL}, F_{LH}, F_{HL} and F_{HH} to get F_Y .
Step 5: fuse the Cb channels of images A and B by PCA to get F_{Cb}.
Step 6: fuse the Cr channels of images A and B by PCA to get F_{Cr}.
Step7: convert F_Y, F_{Cb}, and F_{Cr} into RGB color space to get the fused image.
End.

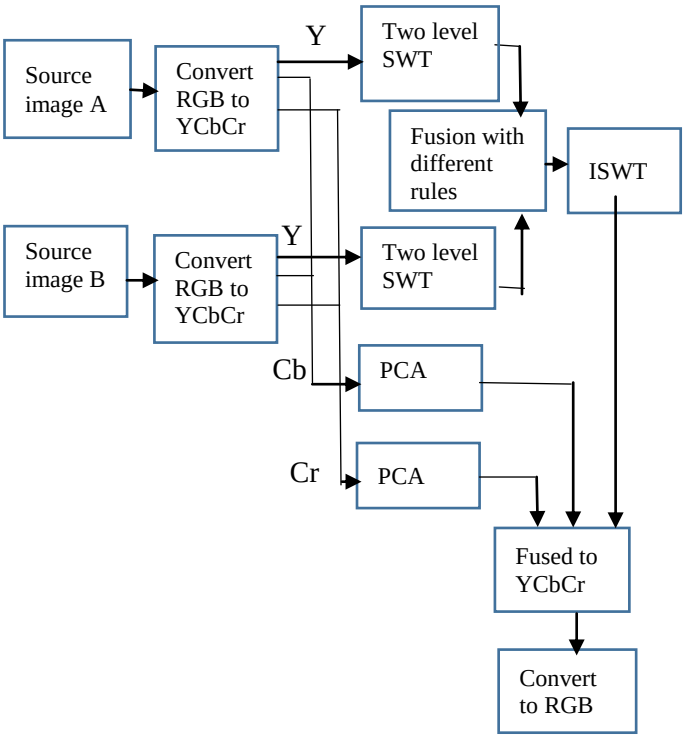

Figure 3. Block diagram of the proposed method

V. Results and Discussion

A. Parametric evaluation

There are several quantitative assessment metrics used to compare various fusion algorithms depending on the reference image. One of them is Root Mean Squared Error (RMSE), which is usually found between the fused image and the original. The smaller the value, then the better the fusion method [16].

$$RMSE \sqrt{\frac{1}{M\times N}\sum_{i=1}^{M}\sum_{j=1}^{N}(R(i,j)-F(i,j))^2} \quad (18)$$

Peak Signal to Noise Ratio (PSNR) is another parametric deployed for fused image quality assessment, which is calculated as:

$$PSNR = 10log_{10}\frac{(M\times N)^2}{\sum_{i=1}^{M}\sum_{j=1}^{N}[R(i,j)-F(i,j)]^2} \quad (19)$$

SSIM is used to calculate the structure similarity between the fused image and the reference one. A better fusion result is indicated by a higher value of PSNR and SSIM [17]. The latter is defined as:

$$SSIM(R,F) = \left(\frac{2\mu_r\mu_f+c_1}{\mu^2{}_r+\mu^2{}_f+c_1}\right)^{\alpha}.\left(\frac{2\sigma_r\sigma_f+c_2}{\sigma^2{}_r+\sigma^2{}_f+c_2}\right)^{\beta}.\left(\frac{\sigma_{rf}+c_3}{\sigma_r\sigma_f+c_3}\right)^{\gamma} \quad (20)$$

where, *R(i, j)* are the pixel values of the reference image, and *F(i, j)* are those of the fused one. The image size is M x N, whilst $\mu_r, \mu_f, \sigma^2{}_r, \sigma^2{}_f, \sigma_{rf}$ are the mean, variance, and covariance, respectively. c_1, c_2, c_3 are constants closing to zero.

B. The results of the proposed method

The proposed method has been implemented on multi focus color images in YCbCr color space. The pixel level image fusion technique is implemented in the spectral and transform domains. Firstly, two levels of SWT were applied on the Y channel of two source images, this being undertaken after many experiments with different levels. A different fuse rule was used to fuse the coefficients of the four sub-bands to reach for appropriate fused rule, while the Cb and Cr channels were fused using PCA. The proposed algorithm was applied on many images of size 256 x 256 , including cars, books and a tree. The reference, source images with right and left focus and the fused images after applying the proposed algorithm are presented in figure (4), figure (5) and figure (6).

Figure 4. Car images. (a) Reference image, (b) image blurred on the right (c) image blurred on the left (d) fused image obtained by the proposed algorithm.

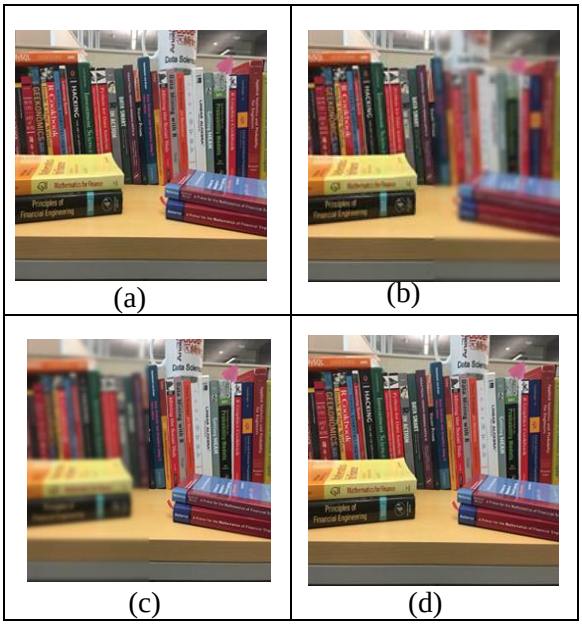

Figure 5. Book images. (a) Reference image, (b) image blurred on the right (c) image blurred on the left (d) fused image obtained by the proposed algorithm.

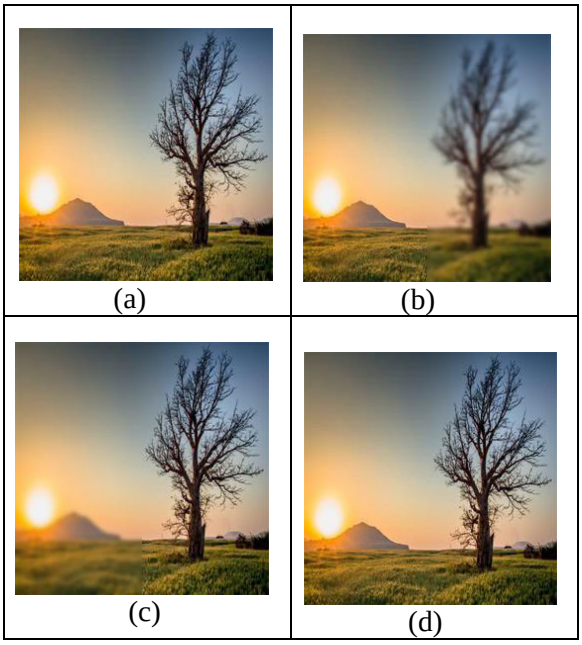

Figure 6. Tree images. (a) Reference image, (b) image blurred on the right (c) image blurred on the left (d) fused image obtained by the proposed algorithm.

In this proposed algorithm the terms of RMSE, PSNR, and SSIM were used to evaluate the performance with respect to reference images. The results were compared to those for other algorithms like fusion by PCA transform applied on YCbCr and RGB color spaces, and fusion with SWT. The results are shown in Tables 1-3.

Table 1.
Performance of fusion methods for the car image

Fusion method	PSNR	RMSE	SSIM
SWT	**33.7300**	**5.2485**	**0.9626**
YCbCr-PCA	**33.7417**	**5.2414**	**0.9866**
RGB-PCA	**35.7091**	**4.1790**	**0.9920**
Proposed method	**38.4651**	**3.0425**	**0.9948**

Table 2.
Performance of fusion methods for the book image

Fusion method	PSNR	RMSE	SSIM
SWT	**32.4733**	**6.0655**	**0.9474**
YCbCr- PCA	**32.9661**	**5.7310**	**0.9844**
RGB-PCA	**34.7795**	**4.6511**	**0.9903**
Proposed method	**39.9168**	**2.5745**	**0.9960**

Table 3.
Performance of fusion methods for the tree image

Fusion method	PSNR	RMSE	SSIM
SWT	**32.4733**	**6.0655**	**0.9474**
YCbCr- PCA	**32.9661**	**5.7310**	**0.9844**
RGB-PCA	**34.7795**	**4.6511**	**0.9903**
Proposed method	**39.9168**	**2.5745**	**0.9960**

The proposed method provides a good visual fused image. It combines the advantages of both the spatial and transform domains. The fused method with the appropriate fuse rules in each sub-band and using PCA for the fused Cb and Cr delivers better performance than the other tested methods.

VI. CONCLUSIONS

In this paper, a fusion method has been proposed in spectral and transform domains at the pixel level. Multi focus source images are converted from RGB into YCbCr color space. The Y channel is decomposed to high frequency and low frequency information by using two level SWT, which was found to be the optimal level after experimentation with others.

To get better results the same fuse rule for approximation sub-band and detail sub-bands is not deployed, i.e., with the proposed algorithm the four sub-bands are fused with a different fusion rule. Moreover, PCA is used to fuse the Cb and Cr channels. It is clear that the proposed

method delivers the best results depending on many referenced measurement criteria. Also the results were compared to the other fusion methods, including PCA transform applied on YCbCr, PCA transform on RGB color space and SWT, to prove higher performance of the proposed algorithm.

REFERENCES

[1] LI, J., YUAN, G., & FAN, H. (2019) Multifocus Image Fusion Using Wavelet-Domain-Based Deep CNN. *Computational Intelligence and Neuroscience*, pp. 1-23. doi: 10.1155/2019/4179397.

[2] AYMAZ, S. and KÖSE, C. (2017) Multi-focus image fusion using Stationary Wavelet Transform (SWT) with Principal Component Analysis (PCA). *Proceedings of the 2017 10th International Conference on Electrical and Electronics Engineering (ELECO)*, Bursa, pp. 1176-1180.

[3] ANCUTI, C.O. and ANCUTI, C., (2013) Single image dehazing by multi-scale fusion. *IEEE Transactions on Image Processing*, 22(8), pp.3271-3282.

[4] WILSON, T.A., ROGERS, S.K. and MYERS, L.R., (1995) Perceptual-based hyperspectral image fusion using multiresolution analysis. *Optical Engineering*, 34(11), pp.3154-3165.

[5] RADHA, N. and BABU, T.R. (2019) Multifocus color image fusion based on walsh Hadamard transform and sum- modified-Laplacian focus measure. *International Journal of Intelligent Engineering and Systems*, 12(1), pp. 142–150. DOI: 10.22266/ijies2019.0228.15

[6] FENG, P. WANG, J. WEI, B. and CHEN, C. (2013) A fusion algorithm for GFP images and phase-contrast images based on Contourlet transform. *Guangdianzi Jiguang/Journal of Optoelectronics Laser*, 24(1), pp. 176–183.

[7] ZHOU, F. LI, X. ZHOU, M. CHEN,Y. and TAN, H.(2019) A new dictionary construction based multimodal medical image fusion framework. *Entropy*, 21(3), article 267, pp. 1-20. doi: 10.3390/e21030267.

[8] HAMED, A.A. AL-SAFAR, A. and TAHA, N.A. (2017) Panchromatic and Multispectral Image Fusion by Combining IHS Transform and Haar Wavelet. *Ibn AL- Haitham Journal For Pure and Applied Science*, 30(3), pp. 236-242. doi: 10.30526/30.3.1624.

[9] KANNAN,K. PERUMAL,A. and ARULMOZHI, K.. (2011) Optimal decomposition level of discrete, stationary and dual tree complex wavelet transform for pixel based fusion of multi-focused images. *Serbian Journal of Electrical Engineering*, 7(1), pp. 81–93.

[10] YANG, T.T. and FANG, P.Y. (2018) Multi exposure image fusion algorithm based on YCbCr space. *IOP Conference Series: Materials Science and Engineering*, 359, 012002, pp/ 1-5. doi:10.1088/1757-899X/359/1/012002

[11] MAZAHERI, S., SULAIMAN, P.S., WIRZA R. , DIMON, M.Z. , KHALID, F. and MOOSAVI TAYEBI, R. (2015) Hybrid pixel-based method for cardiac ultrasound fusion based on integration of PCA and DWT. *Computational and Mathematical Methods in Medicine*, Article ID 486532, pp. 1-16. doi: 10.1155/2015/486532.

[12] LIANFANG, T., AHMED, J., QILIANG, D., SHANKAR, B. and ADNAN, S. (2018). Multi Focus Image Fusion using Combined Median and Average Filter based Hybrid Stationary Wavelet Transform and Principal Component Analysis. *International Journal of Advanced Computer Science and Applications*. 9(6), pp. 34-41. 10.14569/IJACSA.2018.090605.

[13] EHLERS, M., KLONUS, S., JOHAN ÅSTRAND, P. and ROSSO, P. (2010) Multi-sensor image fusion for pansharpening in remote sensing. *International Journal of Image and*

Data Fusion, 1(1), pp.25-45.

[14] JIANG, Q., JIN, X., LEE, S.J., and YAO, S. (2017) A Novel Multi-Focus Image Fusion Method Based on Stationary Wavelet Transform and Local Features of Fuzzy Sets. *IEEE Access*, 5, pp. 20286–20302.

[15] BORWONWATANADELOK, P., RATTANAPITAK, W. and UDOMHUNSAKUL, S., (2009) Multi-focus image fusion based on stationary wavelet transform and extended spatial frequency measurement. *Proceedings of the IEEE 2009 International Conference on Electronic Computer Technology* (pp. 77-81).

[16] NUNEZ, J., OTAZU, X., FORS, O., PRADES, A., PALA, V., and ARBIOL, R. (1999) Multiresolution-based image fusion with additive wavelet decomposition. I*EEE Transactions on Geoscience and Remote sensing*, 37(3), pp. 1204-1211.

[17] YANG, Y. HUANG, S. GAO, J. and QIAN, Z. (2014) Multi-focus image fusion using an effective discrete wavelet transform based algorithm, *Measurement Science Review*, 14(2), pp. 102–108.

参考:

[1] LI J.，YUAN，G. 和 FAN，H.（2019）使用基于小波域的深度 CNN 的多焦点图像融合。计算智能与神经科学，第 1-23 页。 doi：10.1155/2019/4179397。

[2] AYMAZ，S.和 KÖSE，C.（2017）使用固定小波变换（SWT）和主成分分析（PCA）的多焦点图像融合。 2017 年第 10 届电气与电子工程国际会议（ELECO）会议论文集，布尔萨，第 1176-1180 页。

[3] ANCUTI，C.O。和 ANCUTI，C.，（2013）通过多尺度融合进行单个图像去雾。IEEE 图像处理事务，22（8），第 3271-3282 页。

[4] WILSON，T.A.，ROGERS，S.K.和 MYERS，L.R.（1995）使用多分辨率分析的基于感知的高光谱图像融合。光学工程，34（11），第 3154-3165 页。

[5] RADHA，N.和 BABU，T.R.（2019）基于 Walsh-Hadamard 变换和求和修正的 Laplacian 聚焦测量的多焦点彩色图像融合。国际智能工程与系统杂志，12（1），第 142–150 页。 DOI：10.22266/ijies2019.0228.15

[6] FENG，P。Wang，J。WEI，B.和 CHEN，C.（2013）基于 Contourlet 变换的 GFP 图像和相衬图像的融合算法。光电子学报，24（1），第 176–183 页。

[7] ZHOU, F. LI, X. ZHOU, M. CHEN, Y. 和 TAN，H.（2019）一个基于多字典医学图像融合框架的新词典构建。熵，21（3），第 267 条，第 1-20 页。 doi：10.3390/e21030267。

[8] HAMED，A.A.，AL-SAFAR，A.和 TAHA，N.A.（2017）通过结合 IHS 变换和 Haar 小波进行全色和多光谱图像融合。 Ibn AL- Haitham 纯粹与应用科学杂志，30（3），第 236-242 页。 doi：10.30526/0.3.1624。

[9] KANNAN，K。秘鲁和 ARULMOZHI，K.（2011）基于像素的多聚焦图像融合的离散，平稳和对偶树**复**小波变换的最优分解水平。塞尔维亚电气工程杂志，7（1），第 81–93 页。

[10] YANG，T.T. 和 FANG，P.Y.。（2018）基于 YCbCr 空间的多重曝光图像融合算法。 IOP 会议系列：材料科学与工程，359，012002，pp / 1-5。 doi：10.1088/1757-899X/359/1/012002

[11] MAZAHERI, S.，SULAIMAN, P.S.，WIRZA R.，DIMON, M.Z.，KHALID, F。和 MOOSAVI TAYEBI, R.（2015）基于 PCA 和 DWT 集成的基于混合像素的心脏超声融合方法。医学中的计算和数学方法，条款 ID 486532，第 1-16 页。 doi：10.1155/2015/486532。

[12] LIAANGANG，T.，AHMED，J.，QILIANG，D.，SHANKAR，B。和 ADNAN，S。（2018）。基于混合中值和平均滤波器的混合平稳小波变换和主成分分析的多焦点图像融合。国

际高级计算机科学与应用杂志。 9（6），第 34-41 页。 10.14569 / IJACSA.2018.090605。

[13] EHLERS， M.， KLONUS， S.， JOHANÅSTRAND，P.和 ROSSO，P.（2010）多传感器图像融合，用于遥感中的锐化。国际图像和数据融合杂志，1（1），第 25-45 页。

[14] JIANG, Q., JIN, X., LEE, S.J., 和 YAO, S.（2017）一种基于平稳小波变换和模糊集局部特征的新型多焦点图像融合方法。IEEE 访问，5，第 20286-20302 页。

[15] BORWONWATANADELOK， P.， RATTANAPITAK ， W 。 和 UDOMHUNSAKUL，S。，（2009），基于平稳小波变换和扩展空间频率测量的多焦点图像融合。 IEEE 2009 年电子计算机技术国际会议论文集（第 77-81 页）。

[16] NUNEZ，J.，OTAZU，X.，FORS，O.， PRADES， A.， PALA， V. 和 ARBIOL，R.（1999）基于多分辨率的图像融合与加性小波分解。 IEEE 地理科学与遥感学报，37（3），第 1204-1211 页。

[17] YANG, Y. HUANG, S. GAO, J. 和 QIAN, Z.（2014）基于有效离散小波变换的算法的多焦点图像融合，测量科学评论，14（2），第 102-108 页。